

Journal Pre-proof

Near-Infrared Fluorescent Amphiphilic Aza-BODIPY Dye: Synthesis, Solvatochromic Properties, and Selective Detection of Cu²⁺

Jiahe Zuo, Hongfei Pan, Yongjie Zhang, Yuanfang Chen, Houchen Wang, Xiang-Kui Ren, Zhijian Chen

PII: S0143-7208(20)31411-X

DOI: <https://doi.org/10.1016/j.dyepig.2020.108714>

Reference: DYPI 108714

To appear in: *Dyes and Pigments*

Received Date: 5 May 2020

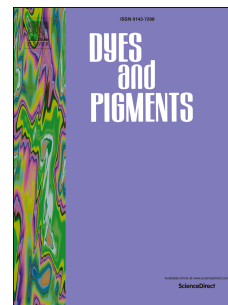
Revised Date: 11 July 2020

Accepted Date: 13 July 2020

Please cite this article as: Zuo J, Pan H, Zhang Y, Chen Y, Wang H, Ren X-K, Chen Z, Near-Infrared Fluorescent Amphiphilic Aza-BODIPY Dye: Synthesis, Solvatochromic Properties, and Selective Detection of Cu²⁺, *Dyes and Pigments*, <https://doi.org/10.1016/j.dyepig.2020.108714>.

This is a PDF file of an article that has undergone enhancements after acceptance, such as the addition of a cover page and metadata, and formatting for readability, but it is not yet the definitive version of record. This version will undergo additional copyediting, typesetting and review before it is published in its final form, but we are providing this version to give early visibility of the article. Please note that, during the production process, errors may be discovered which could affect the content, and all legal disclaimers that apply to the journal pertain.

© 2020 Published by Elsevier Ltd.



Near-Infrared Fluorescent Amphiphilic Aza-BODIPY Dye: Synthesis, Solvatochromic Properties, and Selective Detection of Cu²⁺

Jiahe Zuo, Hongfei Pan, Yongjie Zhang, Yuanfang Chen, Houchen Wang, Xiang-Kui Ren*,
Zhijian Chen*

*School of Chemical Engineering and Technology, Collaborative Innovation Center of Chemistry
Science and Engineering, Tianjin University, Tianjin 300072, China*

Email: zjchen@tju.edu.cn (Z. Chen), renxiangkui@tju.edu.cn (X.-K. Ren)

Abstract

A new amphiphilic near-infrared aza-BODIPY dye bearing both hydrophobic alkyl and hydrophilic oligo-ethylene glycol chains was synthesized by facile click reaction. By introducing the electron-donating *N,N*-disubstituted amino groups into the molecular structure, the new dye show outstanding absorption and fluorescence characteristics, specifically, absorption wavelength up to 850 nm and emission up to 950 nm, and fluorescence quantum yield of 0.29. The solvatochromic properties of the new dye were investigated by UV/Vis absorption and fluorescence spectroscopy. Furthermore, the electrochemical properties of the dye were studied by electrochemical cyclic voltammetry. The application of this dye for the detection of metal ions was further studied. The results indicated selective binding ability of the dye for Cu²⁺ ions and revealed its promising application potential as a near-infrared fluorescence probe.

Keywords: aza-BODIPY; NIR dye; solvatochromism; fluorescence; ion detection

1. Introduction

Over the past decades, organic dyes with absorption and emission in the near-infrared (NIR) region have attracted considerable interests owing to their potential applications in molecular probes, biosensors, phototherapy, and others [1,2]. Up to date, a large number of NIR dyes have been developed, e.g. cyanines [3-5], porphyrins [6,7], phthalocyanines [8-11], squaraines [12], rylene dyes [13,14], and others. Among the NIR dyes, BF₂-chelated azadipyromethenes (aza-BODIPYs) exhibit highly attractive advantages, such as facile synthesis and chemical modification, outstanding optical and electrochemical properties, as well as excellent photostability [15-24]. However, many of the known Aza-BODIPY dyes do not possess absorption and emission above 850 nm [25]. Moreover, this class of dyes are often poorly soluble in polar solvents [26]. These unfavourable features lead to the limitation of application of aza-BODIPYs in various environment. To optimize the optical properties of aza-BODIPY dyes, much efforts have been devoted to shifting the absorption and emission to longer wavelength by structural modifications [21], including attaching strong electron-donating groups [27], extending the conjugation length of the π -systems [3], rigidifying the planarity of dyes [28]. On the other hand, flexible hydrophilic and hydrophobic peripheral chains can be introduced into the molecular structure of the aza-BODIPY dyes to improve their solubility in a wide range of solvents [29-32].

In this paper, we report the design and synthesis of an amphiphilic NIR aza-BODIPY dye with emission wavelength up to 950 nm by introducing *N,N*-dipropargyl groups at the 3,5-phenyl of the aza-BODIPY core and subsequently appending multiple oligo-ethylene glycol (OEG) hydrophilic chains by Cu-catalysed click reaction [33-35]. Noteworthy that such strategy has been successfully in the synthesis of BODIPY-based fluorescent probes by Ng et al. [33] and Wu et al. [36]. In comparison with our previously reported aza-BODIPY dyes [30,37], the absorption and emission bands for the new dye in current work can be largely shifted to longer wavelength by replacement of oxygen atoms at para-positions of 3,5-phenyls with nitrogen. Furthermore, the optical and electrochemical properties of the new NIR dye were investigated and the potential application for metal ion detection was explored.

2. Experimental section

2.1 Materials and Methods

All the reagents and solvents were obtained from commercial suppliers and purified and dried according to standard procedures. Anhydrous dichloromethane (DCM) was distilled over CaH₂ and

THF was distilled over sodium and stored under Argon. Chromatographic purification was performed on silica gel (100 - 200 mesh) columns with the eluents.

^1H NMR and ^{13}C NMR spectra were recorded on Bruker 400MHz NMR spectrometer using chloroform-d as solvent and TMS as an internal standard for the calibration of chemical shifts. High-resolution mass spectrum (HRMS) measurements were performed on a miorOTOF-QII mass spectrometer. UV/Vis absorption spectra were recorded on an Agilent Technologies Cary 300 UV/Vis spectrometer. The spectra were recorded by using quartz glass cuvettes and the absorption coefficient (ϵ_{dye}) was calculated according to Lambert-Beer's law. The electrochemical

The steady state fluorescence spectra and fluorescence quantum yield were measured on an Edinburgh FLS980 spectrofluorometer equipped with an integrating sphere. All the fluorescence spectra were corrected. The time-resolved fluorescence spectroscopic measurement for the dye solution was performed on an Edinburgh FLS980 spectrofluorometer. The instrument response function was collected by scattering the exciting light with the aqueous suspension of Silica (LUDOX). The least square regression analysis of the fluorescence decay curve was performed by the software supplied with the instrument. The quality of the fit was evaluated by analysis of χ^2 (0.9 – 1.1), as well as by inspection of residuals and autocorrelation function.

2.2 Studies on detection of metal ions

The stock solutions of metal ions of Cu^{2+} (CuCl_2), Co^{2+} ($\text{Co}(\text{NO}_3)_2 \cdot 6\text{H}_2\text{O}$), Mg^{2+} ($\text{Mg}(\text{ClO}_4)_2$), Na^+ ($\text{C}_2\text{H}_5\text{ONa}$), Ba^{2+} ($\text{Ba}(\text{ClO}_4)_2$), Cd^{2+} ($\text{Cd}(\text{NO}_3)_2$), Cr^{2+} ($\text{CrCl}_3 \cdot 6\text{H}_2\text{O}$), K^+ (KCl), Mn^{2+} (MnCl_2), Hg^{2+} (HgCl_2), Pb^{2+} ($\text{Pb}(\text{NO}_3)_2$), Zn^{2+} (ZnCl_2), Ca^{2+} ($\text{CaCl}_2 \cdot 2\text{H}_2\text{O}$), and Ni^{2+} ($\text{Ni}(\text{NO}_3)_2$) as well as the stock solution of dye **1** in $\text{CH}_3\text{CN}/\text{H}_2\text{O}$ (1:1 v/v) were prepared and used in the experiments.

For the determination of binding constant (K) between Cu^{2+} and the dye **1**, solutions of Cu^{2+} (1.0 mL) of various concentrations (up to 1.2×10^{-4} M) in $\text{CH}_3\text{CN}/\text{H}_2\text{O}$ (1:1 v/v) were prepared and added to the solutions of dye **1** (1.0 mL) in $\text{CH}_3\text{CN}/\text{H}_2\text{O}$ (1:1 v/v) and spectral changes were monitored by absorption and fluorescence spectroscopy. The values of K were determined by linear least-squares analysis of the absorption spectroscopic data by using equation (1) for 1:2 host-guest complexes [38],

$$\frac{[\text{H}]_0[\text{G}]_0^2}{\Delta A} = \frac{1}{\Delta \epsilon_a K} + \frac{[\text{G}]_0([\text{G}]_0 + 4[\text{H}]_0)}{\Delta \epsilon_a} \quad (1)$$

where $[\text{H}]_0$ and $[\text{G}]_0$ are the initial concentrations of the host and guest, respectively, and ΔA and $\Delta \epsilon_a$ denote changes in the absorbance and molar absorption coefficient, respectively, of the host upon complexation with the guest. The binding constant (K) was determined by the linear fitting of $[\text{H}]_0[\text{G}]_0^2/\Delta A$ against $[\text{G}]_0([\text{G}]_0 + 4[\text{H}]_0)$.

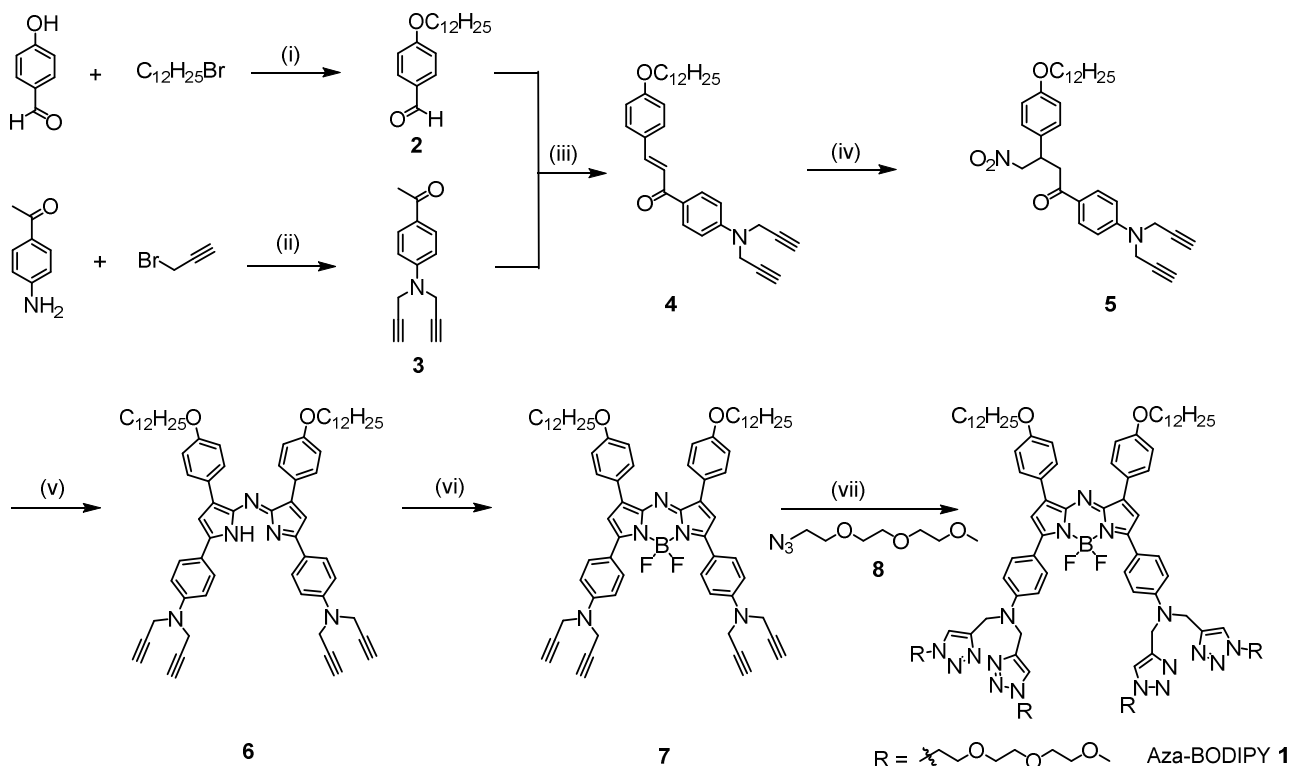
The synthesis and characterization of all the intermediate compounds **2-7** were summarized in Supporting Information. Compound **7** (104.8 mg, 0.10 mmol) and CuI (11.4 mg, 0.06 mmol) was dissolved in *N,N*-Diisopropylethylamine (DIEA, 20ml). triethylene glycolhydrophilic chains (151.2mg, 0.80 mmol) was subsequently added to the reaction system. The reaction mixture was heated to 80°C with stirring and refluxed for 24h. The reaction solvent was then removed by vacuum rotary evaporation. The crude product was purified by silica gel column chromatography (MeOH/CH₂Cl₂ = 1/30) to give a fuchsia solid (140.1 mg, 77.6%). ¹H NMR (400 MHz, CDCl₃): δ = 8.06 (d, *J* = 27.5 Hz, 8H, 8ArH), 7.67 (s, 4H, 4-CH-), 6.96 (d, *J* = 7.5 Hz, 10H, 8-ArH, 2-CH-), 4.80 (s, 8H, 4-CH₂-), 4.49 (s, 8H, 4-CH₂-), 4.03 (s, 4H, 2-CH₂-), 3.82 (s, 8H, 4-CH₂-), 3.51 (s, 32H, 16-CH₂-), 3.29 (s, 12H, 4-CH₃), 1.83 (s, 4H, -CH₂-), 1.49 (s, 4H, -CH₂-), 1.28 (s, 32H, 16-CH₂-), 0.88 (s, 6H, 2-CH₃). ¹³C NMR (101MHz, CDCl₃): δ = 159.97, 155.93, 149.60, 144.83, 144.37, 141.06, 131.53, 130.47, 125.46, 123.31, 120.35, 116.44, 114.52, 112.70, 71.79, 70.49, 70.41, 70.39, 69.37, 68.12, 58.89, 50.23, 46.48, 31.90, 29.66, 29.63, 29.61, 29.59, 29.43, 29.34, 29.28, 26.07, 22.67, 14.12. HRMS (ESI): *m/z* calculated for C₉₆H₁₄₀BF₂N₁₇O₁₄Na ([M+Na]), 1828.0758; found 1828.0669 [M+Na]⁺. Elemental analysis: calculated for C₉₆H₁₄₀BF₂N₁₇O₁₄: C 63.88%, H 7.82%, N 13.19%; found: C 63.49%, H 7.65%, N 12.96%. UV/Vis (CH₂Cl₂): λ_{max}(ε_{dye}) = 781 (127000), 540 (55600), 424 (11830), 350 (34110) M⁻¹ cm⁻¹; Fluorescence (CH₂Cl₂): λ_{max} = 836 nm.

3. Results and discussion

3.1 Synthesis

As shown by the synthetic route of aza-BODIPY **1** in Scheme 1, the intermediate chalcone **4** was synthesized through a typical aldol condensation reaction of corresponding aldehyde and ketone. To improve the synthesis and promote reaction yield of **4**, an optimized reaction condition with long reaction time over 48 h was used. The dye precursor **5** was obtained through a Michael addition reaction of chalcone **4** with nitromethane under basic condition. When potassium *t*-butoxide was used as the base, a good yield of 70% for **5** was obtained. In contrast, only yield lower than 10% was observed for the base diethyl amine, which has been frequently used in other addition reaction with nitromethane [39]. The compound **5** was then heated with ammonium acetate under the solventless condition [40] and the crude condensation product was subsequently treated with BF₃·OEt₂ and *N,N*-diisopropylethylamine (DIEA) in anhydrous CH₂Cl₂ at room temperature for 24 h to give the BF₂-chelated compound **7**. In the last step, the copper(I) catalysed CuAAC "click" reaction between the four terminal alkyne units of **7** and azide-substituted OEG **8** [41] was performed to generate the

amphiphilic aza-BODIPY dye **1** [42, 43]. The dye **1** were fully characterized by ^1H NMR, ^{13}C NMR, as well as high-resolution mass spectroscopy (Supporting Information).



Scheme 1. The synthetic route for aza-BODIPY dye **1**. Reagents and conditions: (i) K_2CO_3 , DMF, rt, 18h, 79%; (ii) K_2CO_3 , DMF, N_2 , 80 °C, 60%; (iii) Sodium ethoxide, ethanol, rt, 48 h, 78%; (iv) CH_3NO_2 , ethanol, Potassium tert-butoxide, 80°C, reflux, 12–24 h, 70%; (v) Ammonium acetate, 120 °C, 24 h, 21%; (vi) $\text{BF}_3 \cdot \text{Et}_2\text{O}$, DIEA, CH_2Cl_2 , rt, 12 h, 57%; (vii) CuI, DIEA, CH_2Cl_2 , CH_3CN , 50 °C, 6 h, 77.6%.

3.2 UV/Vis absorption and emission spectroscopic properties

As shown in Figure 1a and Table 1, the UV/Vis absorption spectrum of aza-BODIPY dye **1** exhibited an intensive NIR band up to 850 nm with molar absorption coefficient higher than $10^5 \text{ M}^{-1}\text{cm}^{-1}$, which could be ascribed to the $\text{S}_0\text{-S}_1$ transition of aza-BODIPY **1**. As compared with the absorption band ($\sim 700 \text{ nm}$) of the aza-BODIPY dyes with alkoxy substituents at the para-positions of 3,5-phenyls [30], the absorption band of **1** is largely shifted to the longer wavelength. Obviously, the large bathochromic shift (*ca.* 80 nm) was caused by the strongly electron-donating amino groups at the para-position of 3,5-phenyls. Meanwhile, the dye **1** exhibited longer wavelength of absorption maximum than that for aza-BODIPY **7**. In addition, the dye **1** displayed the second and lower

absorption band between 500 nm and 600 nm, which could be assigned as the S_0-S_2 transition of the aza-BODIPY dyes [44].

Furthermore, the emission in NIR region was observed for aza-BODIPY dye **1**. The fluorescence spectrum of **1** in dichloromethane have an approximate mirror-image relationship with their S_0-S_1 absorption bands (Figure 1a). The emission maximum of dye **1** was observed at the 836 nm. Meanwhile, a fluorescence quantum yield of 0.29 was determined for the dyes **1**. In the time-resolved fluorescence spectroscopic studies (Figure 1b), the dye **1** showed a bi-exponential fluorescence decay with an averaged fluorescence lifetime ($\langle \tau \rangle$) of 2.7 ns (Table 1).

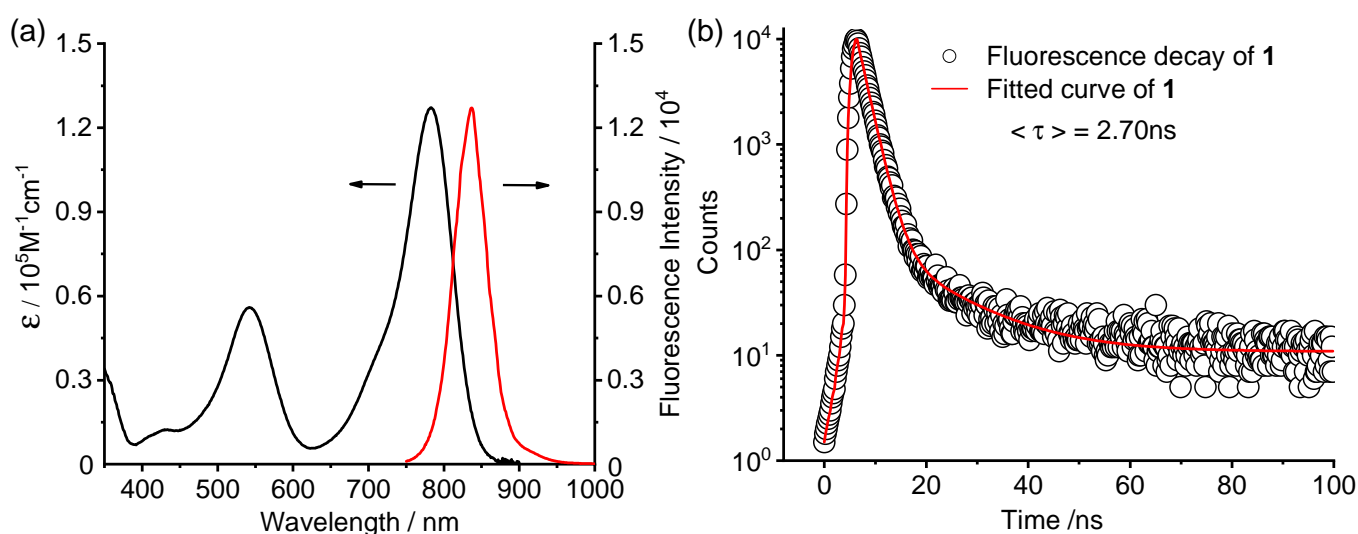


Figure 1. (a) UV/Vis absorption (black line) and fluorescence spectra (red lines) of aza-BODIPY dyes **1** in CH_2Cl_2 , $\lambda_{\text{ex}} = 540$ nm, $[\mathbf{1}] = 5.0 \times 10^{-6}$ M. (b) Fluorescence decay of aza-BODIPY **1** in CH_2Cl_2 , $\lambda_{\text{ex}} = 540$ nm. $\lambda_{\text{em}} = 838$ nm. $[\mathbf{1}] = 5.0 \times 10^{-6}$ M.

Table 1. The absorption maximum (λ_A), absorption coefficient (ϵ_{dye}), emission maximum (λ_F), fluorescence quantum yields (Φ), and fluorescence lifetimes (τ) of the aza-BODIPY dye **1** and **7** in dichloromethane, $[\mathbf{1}] = [\mathbf{7}] = 5.0 \times 10^{-6}$ M.

dye	λ_A/nm	$\epsilon_{\text{dye}}/\text{M}^{-1}\text{cm}^{-1}$	λ_F/nm	Φ^a	$\langle \tau \rangle^b/\text{ns}$	τ_1^c/ns	τ_2^c/ns
1	781	1.3×10^5	836	0.29	2.7	1.9 (92.81%)	12.4 (7.19%)
7	743	1.1×10^5	809	0.28	3.6	2.7 (87.85%)	10.2 (12.15%)

^a Determined by fluorescence spectrometer equipped with integrating sphere.

^b Averaged fluorescence lifetimes.

^c Bi-exponential fluorescence lifetimes and pre-exponential factors (in brackets).

3.3 Solvatochromic Properties

The dye **1** is well-soluble in a number of common organic solvents. To investigate the solvatochromic properties of dye **1**, their absorption and fluorescence spectra were measured in various solvents. Upon the variation in solvent polarity, obvious shift of the absorption and emission bands of **1** was observed (Figure 2a, b). On the other hand, aza-BODIPY **1** display different light-emitting color coordinates in CIE 1931 chromaticity diagram in various polar solvents (Figure S17), indicating that the emission properties of dyes **1** are sensitive to the solvent polarity. In the most polar solvent MeOH, the shortest wavelength of the absorption maximum of 773 nm and the emission maximum of 832 nm were observed (Table 2). With decrease in the solvent polarity, the absorption and emission maxima of the dye **1** were shift bathochromically to longer wavelengths, implying that the dipolemoment of ground state is larger than that of excited state. This result is comparable with the negative solvatochromism reported for BODIPY dyes [45,46]. Based on the optical spectroscopic data summarized in Table 2, the solvatochromism of dye **1** was further quantified by linear free energy relationships (LFER) with Lippert-Mataga equation (2) [47,48],

$$hc(\nu_A - \nu_F) = 2\Delta f \frac{(\mu_E - \mu_G)^2}{a^3} + C \quad (2)$$

where ν_A and ν_F are the wavenumbers (cm^{-1}) of the absorption and emission maxima of dye **1**, respectively, μ_G and μ_E are respectively the dipolemoments of the fluorophore in the ground state and the excited state, h is Planck's constant, c is the speed of light, a is the radius of the cavity in which the fluorophore resides, and Δf is the solvent parameter and can be defined as $[(\epsilon-1)/(2\epsilon+1)] - [(n^2-1)/(2n^2+1)]$. As shown in Figure 2c, an approximate linear relationship of the Stokes shifts and the solvent parameter was observed for dye **1**. According to the linear fitting, the slope $(2/hc)[(\mu_E - \mu_G)^2/a^3]$ was obtained.[48] The cavity radius of the chromophore a was estimated to be 0.58 nm based on molecular modelling. Accordingly, the dipole moments changes between excited and ground states were obtained as -2.1 D for dyes **1**.

Table 2. Stokes' Shifts ($\nu_A - \nu_F / \text{cm}^{-1}$) in various polar solvents (aza-BODIPY **1** = $5.0 \times 10^{-6}\text{M}$).

Solvent	ϵ	n	$\Delta f^{a)}$	λ_A / nm	λ_F / nm	$\nu_A - \nu_F / \text{cm}^{-1}$	$\lambda_F - \lambda_A / \text{nm}$
Methanol	32.66	1.328	0.308	773	832	917	59
Chloroform	4.89	1.446	0.150	776	834	896	58
Dichloromethane	8.93	1.424	0.218	780	837	873	57
Ethyl acetate	6.02	1.372	0.200	782	838	855	56
Acetonitrile	35.94	1.344	0.305	785	842	862	57
Toluene	2.38	1.497	0.015	786	839	803	53
Tetrahydrofuran	7.58	1.407	0.210	790	846	837	56

$$^a \Delta f = [(\epsilon-1)/(2\epsilon+1)] - [(n^2-1)/(2n^2+1)]$$

Moreover, the solvatochromism of dye **1** was also investigated by using empirical solvent polarity parameters, such as ET(30), π^* , and χ_R (Figure S18). The latter is less common and was first reported by Brooker et al. based on their solvatochromic studies for a polymethine dye [49]. Among these polarity scales, the χ_R exhibit good linear free energy relationship for all the 7 solvents (correlation coefficient $R = 0.917$). In comparison with the fitting obtained from the Lippert equation, the correlation is largely improved.

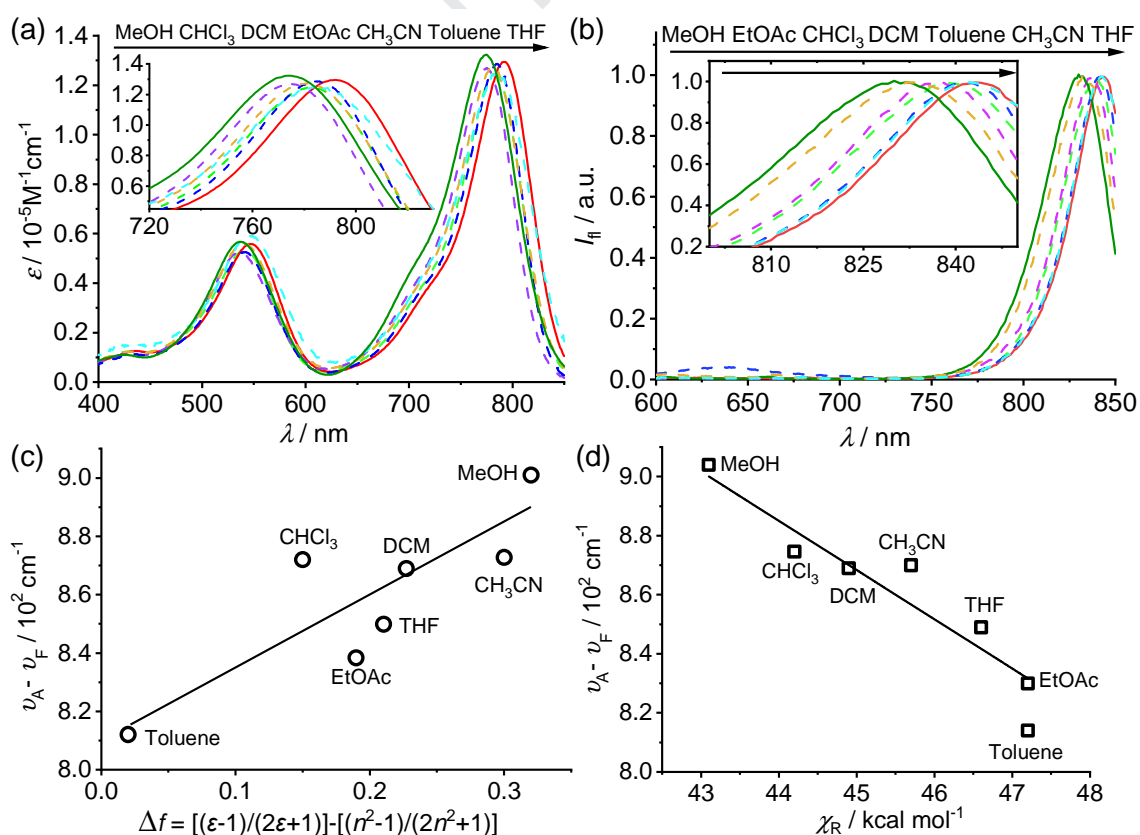


Figure 2. UV/Vis absorption (a) and fluorescence spectra (b) of aza-BODIPY **1** in various solvents, including chloroform (CHCl_3), methanol (MeOH), Acetonitrile (CH_3CN), dichloromethane (DCM),

ethyl acetate (EtOAc), tetrahydrofuran (THF), and toluene. [1] = 5.0×10^{-6} M, $\lambda_{\text{ex}} = 540$ nm. (c) Lippert plots for aza-BODIPY **1** in various solvents. (d) Plot of $(\nu_{\text{A}} - \nu_{\text{F}})$ of aza-BODIPY **1** vs. empirical solvent polarity parameter χ_{R} of different solvents.

For further understanding the excited state properties of these dyes, their redox properties were studied by cyclic voltammetry (CV). The cyclic voltammogram of dye **1** exhibited one reduction peaks at -0.88 V and the first and second oxidation peaks at 0.72 V and 0.98 V (Figure 3). According to the oxidation and reduction potentials obtained from CV measurements, the highest occupied molecular orbital (HOMO) and lowest unoccupied molecular orbital (LUMO) energy levels of the aza-BODIPYs were calculated (Table 3) based on the energy levels of reference Fc/Fc+ (4.78 eV vs. the vacuum level). HOMO/LUMO bandgaps of dye **1** was thus obtained to be 1.60 eV which are generally smaller than the most of previously reported dyes. In comparison with the unsubstituted 1,3,5,7-tetraphenyl aza-BODIPY ($E_{1/2}^{\text{ox}} = 0.90$ V, $E_{1/2}^{\text{red}} = -0.77$ V) [50], the first oxidation potential of aza-BODIPY **1** was cathodically shifted about 0.35 V and the reduction potential was anodically shifted about 0.11 V. Accordingly, a smaller HOMO/LUMO bandgap of 1.21 eV was obtained for the dye **1**. The oxidation potential of dye **1** is also lower than that for 1,3,5,7-tetraphenyl aza-BODIPY bearing methoxy groups [51] or the aza-BODIPYs bearing extended conjugated systems [39,52,53]. Obviously, the electrochemical oxidation of dye **1** was facilitated by the electron-donating amino substituent at the para-position of the 3,5-phenyls.

The small HOMO/LUMO bandgap of dye **1** implies that intramolecular charge transfer may easily occur for this dye molecule. On the basis of redox potentials measured by cyclic voltammetry, the free energy change (ΔG) for the photoinduced charge transfer of dye **1** could be calculated according to the Weller equation (3) [54],

$$\Delta G = E_{\text{ox}}(\text{D}) - E_{\text{red}}(\text{A}) - E_{00}(\text{D}^*) - C \quad (3)$$

where $E_{\text{ox}}(\text{D})$ is the oxidation potential of donor, $E_{\text{red}}(\text{A})$ is the reduction potential of acceptor, $E_{00}(\text{D}^*)$ (eV) is the 0-0 transition energy of the electron donor, which was determined to be 1.53 eV for **1** by [55], and C (0.06 eV or 5.85 KJ/mol) is the stabilization energy of ion solvation. Based on the data in Table 3, the free energy changes of intramolecular charge transfer of **1** was calculated as $\Delta G = -0.30$ eV. The negative value of ΔG indicates that charge transfer processes is thermodynamically feasible upon photoexcitation, which may lead to the longer absorption wavelength of dye **1** in comparison with that for 1,3,5,7-tetraphenyl aza-BODIPYs with the less electron-donating alkoxy substituents at 3,5-phenyls.

Table 3. Oxidation potentials ($E_{\text{ox}}(\text{D})$), reduction potentials ($E_{\text{red}}(\text{A})$), free energy change (ΔG), highest occupied molecular orbital (HOMO) and lowest unoccupied molecular orbital (LUMO)

energy levels of the dye **1**.

$E_{1/2}^{OX}(D)^a$	$E_{1/2}^{red}(A)^a$	HOMO ^b	LUMO ^b	ΔE_g^c
/V	/V	/eV	/eV	/eV
0.55, 0.81	-0.66	-5.33	-4.12	1.21

^aFirst reduction/oxidation potential relative to an internal ferrocene reference. ^bCalculated from the oxidation potential and the reduction potentials by using ferrocene as a reference (-4.78 eV). ^c $\Delta E_g =$ LUMO - HOMO.

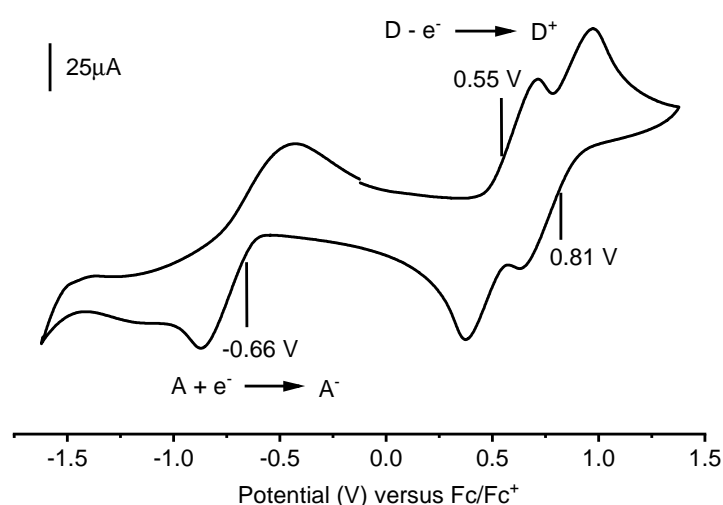


Figure. 3 Cyclic voltammogram of aza-BODIPY **1** in dichloromethane. The scan rate is 100 mV s^{-1} , $[1] = 5.0 \times 10^{-3} \text{ M}$.

3.4 Studies on selective detection of Cu^{2+} ions

It has been reported in literatures [33] that the bis(1,2,3-triazole) amino moieties in BODIPY dyes could be used as a ligand for metal ion detection. Accordingly, the dye **1** was investigated as a new near-infrared fluorescence sensor for the detection of metal ions. As shown in Figure 4a, various metal ions in $\text{CH}_3\text{CN}/\text{H}_2\text{O}$ (1:1 v/v) with a concentration of $2.0 \times 10^{-4} \text{ M}$, including Cu^{2+} (CuCl_2), Co^{2+} ($\text{Co}(\text{NO}_3)_2 \cdot 6\text{H}_2\text{O}$), Mg^{2+} ($\text{Mg}(\text{ClO}_4)_2$), Na^+ ($\text{C}_2\text{H}_5\text{ONa}$), Ba^{2+} ($\text{Ba}(\text{ClO}_4)_2$), Cd^{2+} ($\text{Cd}(\text{NO}_3)_2$), Cr^{2+} ($\text{CrCl}_3 \cdot 6\text{H}_2\text{O}$), K^+ (KCl), Mn^{2+} (MnCl_2), Pb^{2+} ($\text{Pb}(\text{NO}_3)_2$), Zn^{2+} (ZnCl_2), Hg^{2+} (HgCl_2), Ca^{2+} ($\text{CaCl}_2 \cdot 2\text{H}_2\text{O}$), and Ni^{2+} ($\text{Ni}(\text{NO}_3)_2$), were mixed with the dye **1** solution ($5.0 \times 10^{-6} \text{ M}$) in equal volume and spectral changes were monitored by absorption and fluorescence spectroscopy. For Cu^{2+} , the absorption band was significantly blue shifted by 50-55 nm from 784 nm while for the other ions

the absorption spectra displayed almost no changes in comparison with that for pure dye **1**. Moreover, the fluorescence spectra indicated that significant fluorescence quenching took place upon the addition of Cu^{2+} while the fluorescence intensity was remained for the other ions. These results are indicative for the selective sensitivity of dye **1** towards Cu^{2+} .

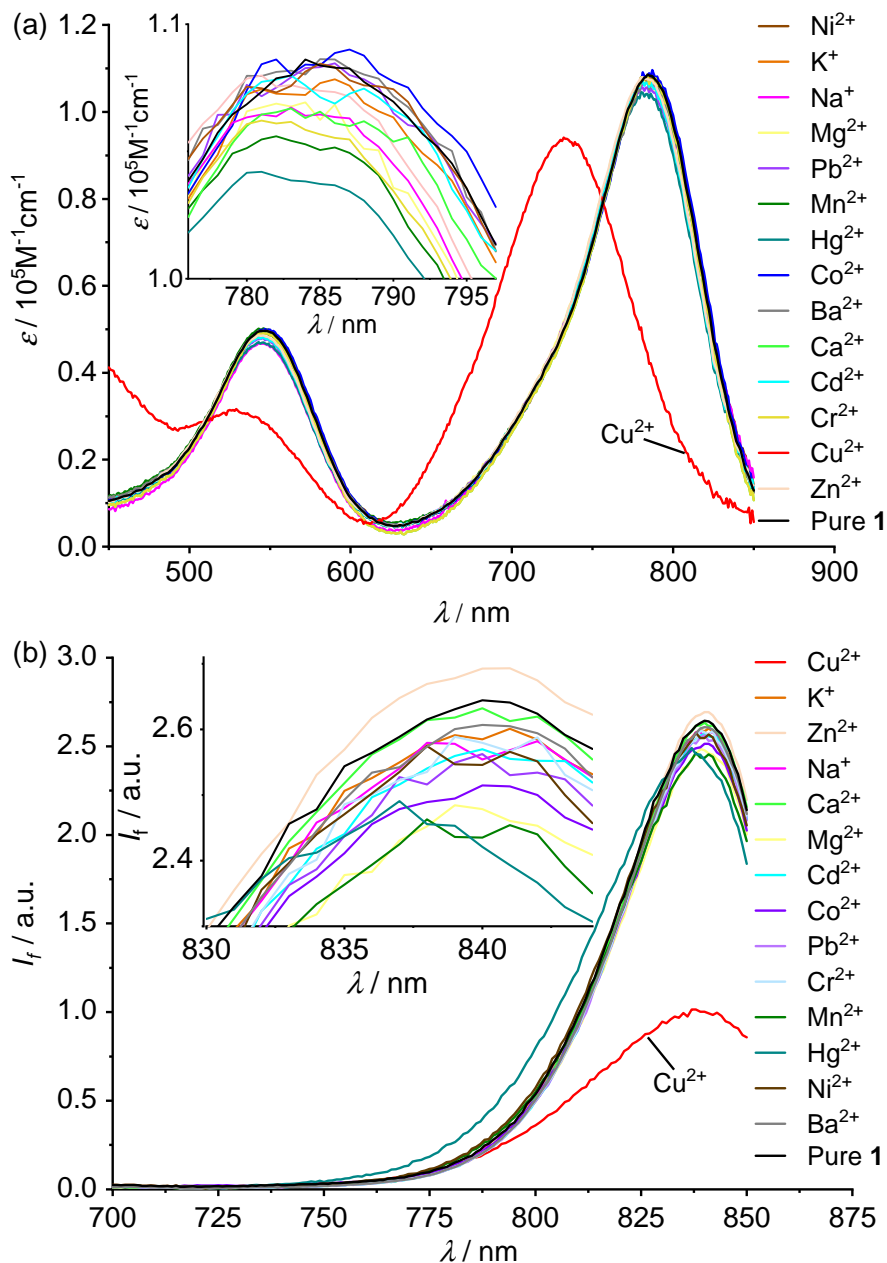


Figure 4. (a) UV/Vis absorption spectra of **1** in $\text{CH}_3\text{CN}/\text{H}_2\text{O}$ (1:1 v/v) upon addition of 20 equivalents of different metal ions. $[\mathbf{1}] = 5.0 \times 10^{-6} \text{ M}$, $[\text{metal ion}] = 1.0 \times 10^{-4} \text{ M}$. Inset: Local enlargement of UV/Vis absorption spectra. (b) Fluorescence spectra of **1** in $\text{CH}_3\text{CN}/\text{H}_2\text{O}$ (1:1 v/v) upon addition of 20 equivalents of different metal ions. $\lambda_{\text{ex}} = 540 \text{ nm}$. $[\mathbf{1}] = 5.0 \times 10^{-6} \text{ M}$, $[\text{metal ion}] = 1.0 \times 10^{-4} \text{ M}$. Inset: Local enlargement of fluorescence spectra.

To further quantitative study the binding properties of dye **1** with Cu²⁺ ions, the dye **1** solution in CH₃CN/H₂O (1:1 v/v) was titrated with Cu²⁺ of various concentrations (Figure 5a). Upon gradual addition of Cu²⁺ up to 24 equivalents, the absorption band of aza-BODIPY **1** is gradually blue-shifted from 785 to 733 nm. Note that the absorption wavelength of 733 nm after the binding of Cu²⁺ is comparable to that for the previously reported aza-BODIPYs dyes without amino substituents [30], indicating that the electron-donating effect of amino group on the absorption was eliminated by the Cu²⁺ binding. Meanwhile, the fluorescence intensity of **1** decreased gradually upon addition of Cu²⁺ at both 20 °C (Figure 5b) and 40 °C (Figure S19). It can be deduced that each of the bis(1,2,3-triazole)amino moiety of **1** binds to one Cu²⁺[33]. This was further evidenced by a Job's plot in Figure S20, which indicated clearly a binding stoichiometry of 1:2 between dye **1** and Cu²⁺. By applying the 1:2 binding model in literature [38], the binding constant between Cu²⁺ and dye **1** was calculated to be $K = (1.6 \pm 0.8) \times 10^9 \text{ M}^{-2}$ through linear least-squares fitting of the change in absorbance at 781 nm. Moreover, the limit of detection of dye **1** for Cu²⁺ was determined to be 1.38 μM, as shown in Figure S21.

The fluorescence quenching data at 20 °C and 40 °C was further analysed by using the Stern-Volmer equation (4) [47],

$$I_0/I_f = 1 + k_q\tau_0[\text{Cu}^{2+}] \quad (4)$$

where I_0 and τ_0 are the intensity and lifetime of dye **1**, and I_f is the fluorescence intensity after addition of Cu²⁺. As shown in the figure 5b, linear relationship was obtained for the quenching data for different temperatures. In general, for dynamic collision quenching, the slope of Stern-Volmer curve increases with increase in temperature. On the other hand, opposite trend has been observed for static chelation quenching[48] since the binding strength between metal ion and ligand become lower upon elevation of temperature. In the case of dye **1**, the higher slope of the Stern-Volmer curve at 20 °C confirmed the static fluorescence quenching by chelation interaction between Cu²⁺ and the bis(1,2,3-triazole) amino groups. In addition, the competition experiments between Cu²⁺ and other metal ions were monitored by fluorescence spectroscopy upon addition of 10 equiv. of other metal ions into a solution containing dye **1** ($5.0 \times 10^{-6} \text{ M}$) and Cu²⁺ ions ($5.0 \times 10^{-5} \text{ M}$, 10 equiv.) in CH₃CN/H₂O (1:1 v/v). As shown in Figure S22, the Cu²⁺ could not be replaced by other metal ions from the complex. This result confirmed the highly selectivity in the recognition and detection of Cu²⁺ by dye **1**.

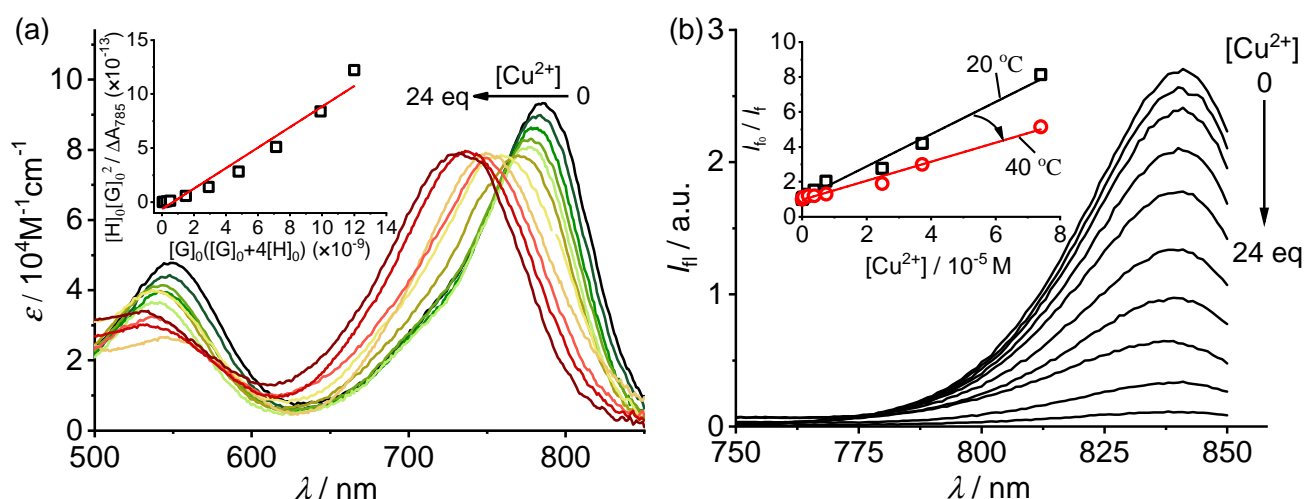


Figure 5. (a) UV/Vis absorption spectra of aza-BODIPY **1** in CH₃CN/H₂O (1:1 v/v) upon the addition of Cu²⁺, [**1**] = 5.0×10⁻⁶ M. Inset: Linear fitting to calculate the binding constant *K* between Cu²⁺ and **1**. (b) Fluorescence spectra of aza-BODIPY **1** in CH₃CN/H₂O (1:1 v/v) upon the addition of Cu²⁺ at 20 °C, [**1**] = 5.0 ×10⁻⁶ M, λ_{ex} = 540 nm. Inset: Stern-Volmer plots of the fluorescence quenching at 20 °C (black) and 40 °C (red).

4. Conclusion

In summary, a new amphiphilic NIR fluorescent aza-BODIPY dye **1** bearing two dodecyloxy hydrophobic chains and four oligo-ethylene glycol hydrophilic chains was facilely synthesized by copper-catalysed click reaction and fully characterized. By introducing the electron-donating *N,N*-disubstituted amino groups at the para-position of the 3,5-phenyls, the dye **1** exhibited absorption wavelength up to 850 nm and emission wavelength up to 950 nm. The solvent-dependent UV/Vis and fluorescence spectroscopic studies indicated the absorption and emission wavelengths of the dye **1** are sensitive to the environmental polarity and the negative solvatochromism was observed. Electrochemical studies revealed that intramolecular charge transfer is feasible for dye **1** and may cause the longer absorption wavelength of this dye than that for the aza-BODIPYs bearing alkoxy substituents at 3,5-phenyls. Furthermore, the bis(1,2,3-triazole) amino moiety in dye **1** can selectively response and binding to Cu²⁺ among the studied 15 different metal ions. Accordingly, the dye **1** exhibited promising application potential as a new near-infrared fluorescence probe for Cu²⁺.

Acknowledgements

We acknowledge National Natural Science Foundation of China (No. 21676186 and No. 21875157), the Tianjin Research Program of Application Foundation and Advanced Technology (No.

Supplementary data

Supplementary data to this article can be found online.

References

- [1] Yuan L, Lin W, Zheng K, He L, Huang W. Far-red to near infrared analyte-responsive fluorescent probes based on organic fluorophore platforms for fluorescence imaging. *Chem Soc Rev.* 2013;42(2):622-61.
- [2] Zhao W, Carreira EM. Conformationally Restricted Aza-BODIPY: Highly Fluorescent, Stable Near-Infrared Absorbing Dyes. *Chem-eur J.* 2006;12(27):7254-63.
- [3] Cui J, Sheng W, Wu Q, Yu C, Hao E, Bobadova-Parvanova P, Storer M, Asiri AM, Marwani HM, Jiao L. Synthesis, Structure, and Properties of Near-Infrared [b]Phenanthrene-Fused BF₂ Azadipyrrromethenes. *Chem Asian J.* 2017;12(18):2486-93.
- [4] Peng X, Song F, Lu E, Wang Y, Zhou W, Fan J, Gao Y. Heptamethine Cyanine Dyes with a Large Stokes Shift and Strong Fluorescence: A Paradigm for Excited-State Intramolecular Charge Transfer. *J Am Chem Soc.* 2005;127(12):4170-1.
- [5] Shindy HA. Fundamentals in the chemistry of cyanine dyes: A review. *Dyes Pigments.* 2017;145:505-13.
- [6] Loudet A, Bandichhor R, Wu L, Burgess K. Functionalized BF₂ Chelated Azadipyrrromethene Dyes. *Tetrahedron.* 2008;64(17):3642-54.
- [7] Sprafke JK, Stranks SD, Warner JH, Nicholas RJ, Anderson HL. Noncovalent Binding of Carbon Nanotubes by Porphyrin Oligomers. *Angew Chem Int Edit.* 2011;50(10):2313-6.
- [8] Rodríguez-Morgade MS, Planells M, Torres T, Ballester P, Palomares E. A colorimetric molecular probe for Cu(II) ions based on the redox properties of Ru(II) phthalocyanines. *J Mater Chem.* 2008;18(2):176-81.
- [9] Lo PC, Huang JD, Cheng DY, Chan EY, Fong WP, Ko WH, Ng DKP. New amphiphilic silicon(IV) phthalocyanines as efficient photosensitizers for photodynamic therapy: synthesis, photophysical properties, and in vitro photodynamic activities. *Chem-eur J.* 2004;10(19):4831-8.
- [10] Lin MJ, Wang JD, Chen NS, Huang JL. A convenient synthesis of a substituted phthalocyanine compound. *J Coord Chem.* 2006;59(6):607-11.
- [11] Chen Y, Zhao S, Li X, Jiang J. Tuning the arrangement of mono-crown ether-substituted phthalocyanines in Langmuir–Blodgett films by the length of alkyl chains and the cation in subphase. *J Colloid Interf Sci.* 2005;289(1):200-5.

- [12] Mayerhoffer U, Deing K, Gruss K, Braunschweig H, Meerholz K, Würthner F. Outstanding short-circuit currents in BHJ solar cells based on NIR-absorbing acceptor-substituted squaraines. *Angew Chem Int Edit.* 2009;48(46):8776-9.
- [13] Heek T, Würthner F, Haag R. Synthesis and Optical Properties of Water-Soluble Polyglycerol-Dendronized Rylene Bisimide Dyes. *Chem- eur J.* 2013;19(33):10911-21.
- [14] Zhang X, Chen Z, Würthner F. Morphology Control of Fluorescent Nanoaggregates by Co-Self-Assembly of Wedge- and Dumbbell-Shaped Amphiphilic Perylene Bisimides. *J Am Chem Soc.* 2007;129(16):4886-7.
- [15] Gresser R, Hummert M, Hartmann H, Leo K, Riede M. Synthesis and Characterization of Near-Infrared Absorbing Benzannulated Aza-BODIPY Dyes. *Chem- eur J.* 2011;17(10):2939-47.
- [16] Jiang X, Zhang T, Sun C, Meng Y, Xiao L. Synthesis of aza-BODIPY dyes bearing the naphthyl groups at 1,7-positions and application for singlet oxygen generation. *Chinese Chem Lett.* 2019;30(5):1055-8.
- [17] Flores O, Pliquet J, Abad Galan L, Lescure R, Denat F, Maury O, Pallier A, Bellaye PS, Collin B, Meme S, Bonnet CS, Bodio E, Goze C. Aza-BODIPY Platform: Toward an Efficient Water-Soluble Bimodal Imaging Probe for MRI and Near-Infrared Fluorescence. *Inorg Chem.* 2020;59(2):1306-14.
- [18] Dolati H, Haufe LC, Denker L, Lorbach A, Grotjahn R, Horner G, Frank R. Two pi-Electrons Make the Difference: From BODIPY to BODIIM Switchable Fluorescent Dyes. *Chem- eur J.* 2020;26(6):1422-8.
- [19] Liu C, Ding W, Liu Y, Zhao H, Cheng X. Self-assembled star-shaped aza-BODIPY mesogen affords white-light emission. *New J Chem.* 2020;44(1):102-9.
- [20] Gawale Y, Mangalath S, Adarsh N, Joseph J, Ramaiah D, Sekar N. Novel Aza-BODIPY based turn on selective and sensitive probe for on-site visual detection of bivalent copper ions. *Dyes Pigments.* 2019;171.
- [21] Zhang X, Yu H, Xiao Y. Replacing Phenyl Ring with Thiophene: An Approach to Longer Wavelength Aza-dipyrrromethene Boron Difluoride (Aza-BODIPY) Dyes. *J Org Chem.* 2012;77(1):669-73.
- [22] Du J, Fan J, Peng X, Li H, Wang J, Sun S. Highly Selective and Anions Controlled Fluorescent Sensor for Hg²⁺ in Aqueous Environment. *J Fluoresc.* 2008;18(5):919-24.
- [23] Pliquet J, Dubois A, Racœur C, Mabrouk N, Amor S, Lescure R, Bettaieb A, Collin B, Bernhard C, Denat F. A promising family of fluorescent water-soluble aza-BODIPY dyes for in vivo molecular imaging. *Bioconjugate Chem.* 2019;30:1061-6.
- [24] Gao Y, Pan Y, He Y, Chen H, Nemykin VN. A fast-response, red emission

Journal Pre-proof
aza-BODIPY-hydrazone-based chemodosimeter for selective detection of HClO. *Sensor Actuat B-chem.* 2018;269:151-7.

- [25] Frimannsson DO, Grossi M, Murtagh J, Paradisi F, O'Shea DF. Light Induced Antimicrobial Properties of a Brominated Boron Difluoride (BF₂) Chelated Tetraarylazadipyrrromethene Photosensitizer. *J Med Chem.* 2010;53(20):7337-43.
- [26] Fan G, Yang L, Chen Z. Water-soluble BODIPY and aza-BODIPY dyes: synthetic progress and applications. *Front Chem Sci Eng.* 2014;8(4):405-17.
- [27] Killoran J, Allen L, Gallagher JF, Gallagher WM, O'Shea DF. Synthesis of BF₂ chelates of tetraarylazadipyrrromethenes and evidence for their photodynamic therapeutic behaviour. *Chem Commun (Camb).* 2002(17):1862-3.
- [28] Yamane H, Ohtani S, Tanaka K, Chujo Y. Synthesis of furan-substituted aza-BODIPYs having near-infrared emission. *Tetrahedron Lett.* 2017;58(30):2989-92.
- [29] Yang L, Fan G, Ren X, Zhao L, Wang J, Chen Z. Aqueous self-assembly of a charged BODIPY amphiphile via nucleation-growth mechanism. *Phys Chem Chem Phys.* 2015;17(14):9167-72.
- [30] Chen Z, Liu Y, Wagner W, Stepanenko V, Würthner F. Near-IR Absorbing J-Aggregate of an Amphiphilic BF₂-Azadipyrrromethene Dye by Kinetic Cooperative Self-Assembly. *Angew Chem.* 2017;56(21):5729-33.
- [31] Liu Y, Zhang Y, Franziska F, Wolfgang W, Frank W, Chen Y, Chen Z. Coupled cooperative supramolecular polymerization: A new model applied to the competing aggregation pathways of an amphiphilic aza-BODIPY dye into spherical and rod-like aggregates. *Chem-eur J.* 2018;24(61):16388-94.
- [32] Wang H, Zhang Y, Chen Y, Pan H, Ren X, Chen Z. Living Supramolecular Polymerization of an Aza-BODIPY Dye Controlled by a Hydrogen-Bond-Accepting Triazole Unit Introduced by Click Chemistry. *Angew Chem Int Ed Engl.* 2020.
- [33] Shi WJ, Liu J, Ng DKP. A Highly Selective Colorimetric and Fluorescent Probe for Cu²⁺ and Hg²⁺ Ions Based on a Distyryl BODIPY with Two Bis(1,2,3-triazole)amino Receptors. *Chem Asian J.* 2012;7(1):196-200.
- [34] Yao Z, Yang Y, Chen X, Hu X, Zhang L, Liu L, Zhao Y, Wu H. Visual Detection of Copper(II) Ions Based on an Anionic Polythiophene Derivative Using Click Chemistry. *Anal Chem.* 2013;85(12):5650-3.
- [35] Zheng H, Li Y, Zhou C, Li Y, Yang W, Zhou W, Zuo Z, Liu H. Synthesis of a [2]Rotaxane Incorporating a "Magic Sulfur Ring" by the Thiol-Ene Click Reaction. *Chem-eur J.* 2011;17(7):2160-7.
- [36] Vedamalai M, Wu SP. A BODIPY-Based Highly Selective Fluorescent Chemosensor for Hg²⁺

- [37] Chen Y, Zhang X, Cheng D, Zhang Y, Liu Y, Ji L, Guo R, Chen H, Ren X, Chen Z, Qiao Z, Wang H. Near-Infrared Laser-Triggered In Situ Dimorphic Transformation of BF₂-Azadipyromethene Nanoaggregates for Enhanced Solid Tumor Penetration. *ACS Nano.* 2020;14(3):3640-50.
- [38] Liu Y, Yu H, Chen Y, Zhao Y. Synthesis of bridged and metallobridged bis(beta-cyclodextrin)s containing fluorescent oxamidobisbenzoyl linkers and their selective binding towards bile salts. *Chem-eur J.* 2006;12(14):3858-68.
- [39] Zhu L, Xie W, Zhao L, Zhang Y, Chen Z. Tetraphenylethylene- and fluorene-functionalized near-infrared aza-BODIPY dyes for living cell imaging. *RSC Adv.* 2017;7(88):55839-45.
- [40] Hall M, McDonnell SO, Killoran J, O'Shea DF. A Modular Synthesis of Unsymmetrical Tetraarylazadipyromethenes. *J Org Chem.* 2005;36(14):5571-8.
- [41] Dan K, Bose N, Ghosh S. Vesicular assembly and thermo-responsive vesicle-to-micelle transition from an amphiphilic random copolymer. *Chem Commun (Camb).* 2011;47(46):12491.
- [42] Liang L, Astruc D. The copper(I)-catalyzed alkyne-azide cycloaddition (CuAAC) "click" reaction and its applications. An overview. *Coordin Chem Rev.* 2011;255(23-24):2933-45.
- [43] Xu L, Li YJ, Li YL. Application of "Click" Chemistry to the Construction of Supramolecular Functional Systems. *Asian J Org Chem.* 2014;3(5):582-602.
- [44] Xiao M, Mao X, Zhang S, Huang X, Cheng Y, Zhu C. Aza-BODIPY-based D- π -A conjugated polymers with tunable band gap: synthesis and near-infrared emission. *Polym Chem-UK.* 2013;4(3):520-7.
- [45] Qin W, Baruah M, Van der Auweraer M, Frans C DS, Boens N. Photophysical Properties of Borondipyromethene Analogues in Solution. *J Phys Chem A.* 2005;109(33):7371-84.
- [46] Qin W, Leen V, Dehaen W, Cui J, Xu C, Tang X, Liu W, Rohand T, Beljonne D, Van Averbeke B, Clifford JN, Driesen K, Binnemans K, Van der Auweraer M, Boens N. 3,5-Dianilino Substituted Difluoroboron Dipyromethene: Synthesis, Spectroscopy, Photophysics, Crystal Structure, Electrochemistry, and Quantum-Chemical Calculations. *J Phys Chem A.* 2009;113:11731-40.
- [47] Lakowicz JR. Principles of fluorescence spectroscopy. Plenum Press. 1983.
- [48] Wang B, Zhang X, Jia X, Li Z, Ji Y, Yang L, Wei Y. Fluorescence and Aggregation Behavior of Poly(amidoamine) Dendrimers Peripherally Modified with Aromatic Chromophores: the Effect of Dendritic Architectures. *J Am Chem Soc.* 2004;126(46):15180-94.
- [49] Brooker LGS, Craig AC, Heseltine DW, Jenkins PW, Lincoln LL. Color and Constitution. XIII. Merocyanines as Solvent Property Indicators. *J Am Chem Soc.* 1965;87(11).
- [50] Mueller T, Gresser R, Leo K, Riede M. Organic solar cells based on a novel infrared absorbing

aza-bodipy dye. *Sol Energ Mat Sol C*. 2012;99:176–81.

- [51] Jiao L, Wu Y, Ding Y, Wang S, Zhang P, Yu C, Wei Y, Mu X, Hao E. Conformationally restricted aza-dipyrrromethene boron difluorides (aza-BODIPYs) with high fluorescent quantum yields. *Chem Asian J*. 2014;9(3):805-10.
- [52] Koch A, Ravikanth M. Monofunctionalized 1,3,5,7-TetraarylazaBODIPYs and Their Application in the Synthesis of AzaBODIPY Based Conjugates. *J Org Chem*. 2019;84(17):10775-84.
- [53] Kumar S, Thorat KG, Ravikanth M. Synthesis and Properties of Covalently Linked Aza-BODIPY-BODIPY Dyads and Aza-BODIPY-(BODIPY)₂ Triads. *J Org Chem*. 2017;82(13):6568-77.
- [54] Knibbe H, Rehm D, Weller A. Intermediates and Kinetics of Fluorescence Quenching by Electron Transfer. *Berichte der Bunsengesellschaft für physikalische Chemie*. 1968;72(2):257-63.
- [55] Sekaran B, Jang Y, Misra R, D'Souza F. Push-Pull Porphyrins via beta-Pyrrole Functionalization: Evidence of Excited State Events Leading to High-Potential Charge-Separated States. *Chem-eur J*. 2019;25(56):12991-3001.

Highlights

- A new amphiphilic NIR aza-BODIPY dye with absorption up to 850 nm and emission up to 950 nm was synthesized.
- The solvatochromic properties of the new dye were investigated.
- The dye can be used for the selective detection of Cu^{2+} ions.

Journal Pre-proof

CRedit author statement

Jiahe Zuo: Investigation, Methodology, Writing - original draft. **Hongfei Pan:** Data curation, Validation. **Yongjie Zhang:** Conceptualization. **Yuanfang Chen:** Formal analysis. **Houchen Wang:** Writing - review & editing. **Xiang-Kui Ren:** Resources, Writing - review & editing, Funding acquisition. **Zhijian Chen:** Conceptualization, Supervision, Resources, Writing - review & editing, Supervision, Funding acquisition.

Declaration of interests

The authors declare that they have no known competing financial interests or personal relationships that could have appeared to influence the work reported in this paper.

The authors declare the following financial interests/personal relationships which may be considered as potential competing interests:

Journal Pre-proof